

# Use of Multi-Coil Arrays for Separation of Signal from Multiple Slices Simultaneously Excited.

DJ Larkman<sup>1</sup>, JV Hajnal<sup>1</sup>, AH Herlihy<sup>1</sup>, GA Coutts<sup>1</sup>, IR Young<sup>1</sup>, G Ehnholm<sup>2</sup>.

<sup>1</sup>The Robert Steiner Magnetic Resonance Imaging Unit, Imperial College School of Medicine, Hammersmith Hospital, Du Cane Road, London W12 0HS. <sup>2</sup>Picker Nordstar, Helsinki, Finland.

**Introduction:** Several authors have attempted to make use of simultaneous multi-slice acquisitions. Achieving such an excitation is relatively simple, the difficulty lies in untangling the resultant image. Previous work has relied on encoding unique phase information into each slice position [1],[2]. This work demonstrates an alternative approach relying on the use of a multi-coil array to provide unique sensitivity information for each slice position. The resultant mixed slice images can be untangled using matrix algebra to solve a set of simultaneous linear equations. Related approaches have been used for decreasing the number of phase encode steps required for conventional image acquisition [3],[4],[5].

**Theory:** The method resolves simultaneously excited slices providing there is a minimum of the same number of coils as slices and each coil has a different sensitivity to any given slice. This sensitivity is spatially dependent and for  $n$  slices with  $n$  coils the total complex signal acquired in coil 1 in a single pixel ( $C_1$ ) is given by the equation:

$$S_{11}x_1 + S_{12}x_2 + S_{13}x_3 + \dots + S_{1n}x_n = C_1 \quad \text{Equation 1}$$

where  $S_{ij}$  is the complex sensitivity of coil  $i$  to slice  $j$ ,  $x_j$  is the spatially dependent complex signal from slice  $j$ , and  $C$  is defined above. Similar expressions for the other coils can be constructed leading to the soluble set of equations expressed in matrix form:

$$\begin{bmatrix} S_{11} & S_{12} & S_{13} & \dots & S_{1n} \\ S_{21} & S_{22} & S_{23} & \dots & S_{2n} \\ S_{31} & S_{32} & S_{33} & \dots & S_{3n} \\ \vdots & \vdots & \vdots & \vdots & \vdots \\ S_{n1} & S_{n2} & S_{n3} & \dots & S_{nm} \end{bmatrix} \begin{bmatrix} x_1 \\ x_2 \\ x_3 \\ \vdots \\ x_n \end{bmatrix} = \begin{bmatrix} C_1 \\ C_2 \\ C_3 \\ \vdots \\ C_n \end{bmatrix} \quad \text{Equation 2}$$

and in shorthand notation:

$$[S][x] = [C] \quad \text{Equation 3}$$

The solution for  $[x]$  is given by:

$$[x] = [S]^{-1} \cdot [C] \quad \text{Equation 4}$$

where  $[S]^{-1}$  is the inverse of the complex sensitivity matrix  $[S]$ . The set of complex matrices  $[x]$  holds the MR signal at each pixel for each slice.

**Method:** A multi-slice excitation was achieved by appropriate modification of a standard sinc profiled pulse, such that a discrete set of slices could be excited. This work was performed with a four-slice excitation and a four receive coil linear spine array. The slice positions were not commensurate with the coil spacing as this is not a methodological requirement.

The complex sensitivity matrix was generated empirically from four acquisitions. Each acquisition excited a single transverse slice in a large uniform phantom, one at each of the four positions at which the multi-slice excitation operated. These data then contain the sensitivity of each coil to a single slice at each position and this information provides the complex  $4 \times 4$  array ( $[S]$  above) for each pixel within the area covered by the uniform phantom. These data need only be acquired once for a given geometry of coils and slices.

Full simultaneous four slice data was acquired with four cylindrical samples one placed at each of the four slice positions.

The inverse complex sensitivity matrix for each pixel was calculated using Gaussian elimination. This and all other image manipulation was performed using IDL (Research Systems, Colorado) running on a DEC Alpha workstation.

All imaging was performed on a 0.5T Picker Asset scanner. The sensitivity matrix acquisitions and imaging acquisitions were all simple gradient echo sequences with  $128 \times 256$  matrix, field of view 26cm, TR/TE 8.1/400 and 2 sample averages, total acquisition time 102s

**Results:** Uncorrected magnitude images of the test phantoms from a four slice simultaneously acquired data set can be seen in figure 1A, (coils 1-4).

Pixel by pixel corrected magnitude images are shown in figure 1B (coils 1-4). The uncorrected images show the mixed data (the magnitude of array  $[C]$ ) and the corrected images have appropriately redistributed data (magnitude of array  $[x]$ ). Both sets of images have been windowed and levelled in the same way. Figure 2 shows a single line profile through the magnitude image acquired by coil 4, A, before correction and B, after correction.

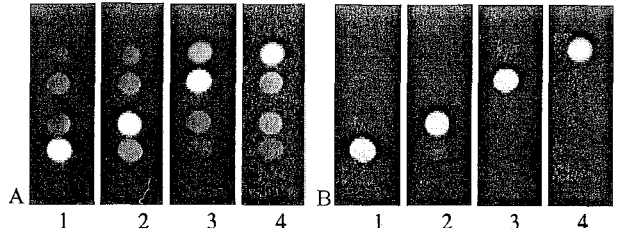


**Figure 1:** Uncorrected data from coils 1 to 4 can be seen in the four images on the left with corrected data on the right. Both sets of images have been windowed and levelled in the same way

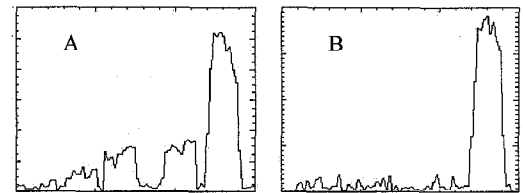


**Figure 2:** A single line of uncorrected data from coil 4 can be seen in A with the same line of corrected data from coil 4 in B.

**Discussion:** We have demonstrated the application of this technique for resolving four slice images with a four-coil array. For  $n$  coils the principle holds for  $\leq n$  slices. The limitation is that each coil must have sufficiently different complex sensitivity to each slice for the matrix equation 3 not to become ill-conditioned. For the principle to be generally useful the whole volume of coil sensitivity can be mapped, once this is done oblique slices in any orientation which satisfy the above criteria can be resolved assuming the coil geometry is fixed.

Signal to noise in such processing is critically dependent on the noise in the array sensitivity matrix  $[S]$ . Zero noise in  $[S]$  means the pure combination of uncorrelated noise with correlated signal, which would produce a net improvement in SNR. In reality as  $[S]$  is obtained empirically there will be noise and this contributes to error in the corrected data.

The principle application of the technique lies in the factor of  $n$  saving in acquisition time for  $n$  slices. Contrast enhanced dynamic scanning, where temporal resolution is paramount, would benefit directly from such an approach. Spine imaging where arrays are routinely used would again benefit by shorter total acquisition times. Further applications involve the elimination of 'fold over' image contamination due to field inhomogeneity. This is particularly relevant in short bore systems where B<sub>0</sub> fringe field distortion can produce a second slice position for a single frequency excitation.

- [1]Souza S.P.,Szumowski J.,Dumoulin C.L.,Plews D.P.,Glover G. J *Comput Assist Tomogr*,12(6), 1026-30, 1988
- [2]Muller S.,*Magn Reson Med*,6(3), 364-71, 1988
- [3]Ra J.B.,Rim C.Y.,*Magn Reson Med*,30(1), 142-45, 1993
- [4]Hutchinson M.,Raff U., *Magn Reson Med*,6(1), 87-91, 1988
- [5]Kwiat D.,Einav S.,Navon G.,*Med Phys*,18(2),251-65, 1991